

## Novel Bioactive and Stable Neurotensin Peptide Analogues Capable of Delivering Radiopharmaceuticals and Molecular Beacons to Tumors

Samuel Achilefu,<sup>\*,†</sup> Ananthacari Srinivasan,<sup>§</sup> Michelle A. Schmidt,<sup>§</sup> Hermo N. Jimenez,<sup>§</sup> Joseph E. Bugaj,<sup>§</sup> and Jack L. Erion<sup>§</sup>

Mallinckrodt Institute of Radiology, Washington University School of Medicine, 4525 Scott Avenue, St. Louis, Missouri 63110 and Mallinckrodt Inc., 675 McDonnell Boulevard, St. Louis, Missouri 63042

Received February 18, 2003

The prevalence of neurotensin receptor (NTR) in several human tumors makes it an attractive target for the delivery of cytotoxic drugs and imaging agents. Native neurotensin (NT) is a tridecapeptide that binds to NTR and induces tumor growth. Unfortunately, NT has a short plasma half-life, which hinders its use for *in vivo* biomedical applications. Numerous reports suggest that Arg(8)-Arg(9) and Tyr(11)-Ile(12) amide bonds are particularly susceptible to degradation by proteolytic enzymes. Predicated on this observation, we substituted Arg(8), Arg(9), and Ile(12) amino acids with the corresponding commercially available mimics. These surrogate amino acids are amenable to standard Fmoc peptide synthesis strategy, and the resulting compounds are stable in biological media for > 4 h and bind to NTR with high affinity. Furthermore, conjugating DTPA to the new peptides and subsequent labeling with <sup>111</sup>In–DTPA for nuclear imaging or fluorescein for optical imaging did not diminish the NTR binding affinities of the peptides. *In vivo* biodistribution of a representative <sup>111</sup>In–DTPA–NT peptide analogue in SCID mice bearing NTR-positive human adenocarcinoma (HT29) xenograft shows that the compound was primarily retained in tumor tissue (2.2% ID/g) and the kidneys (4.8% ID/g) at 4 h postinjection. Coinjection of cold NT and the radiolabeled NT peptide analogue inhibited the tumor but not the kidney uptake, demonstrating that retention of the radiolabeled compound in tumor tissue was mediated by NTR specific uptake while it accumulates in the kidneys by a nonspecific mechanism. These findings show that the new NT peptide analogues are robust and can deliver imaging agents to NTR-positive tumors such as pancreatic cancer.

### Introduction

Incorporating amino acid mimics into the structural framework of bioactive peptides and proteins is a common strategy to stabilize metabolically unstable biomolecules. This approach is particularly important for diagnostic and therapeutic drugs that target the molecular basis of pathogenesis. The neurotransmitter peptide, neurotensin (NT; Figure 1a), is one of such biomolecules. NT is a tridecapeptide that functions as neuromodulator in the central nervous system and has a range of physiological functions in the periphery.<sup>1</sup> Its activity is mediated by interacting with specific G protein-coupled receptors (NTR) to trigger the activation of a cascade of events.<sup>2</sup> Three subtypes of NTR are well characterized, and several studies have demonstrated the up-regulation of these NTRs in various tumors, where NT is known to stimulate the proliferation of cancer cells.<sup>3,4</sup>

The observation that NTR subtype 1 (NTR1) is expressed at high levels in exocrine pancreatic cancer cells suggests the potential utility of NT as a delivery vehicle for diagnostic and cytotoxic drugs to NTR-positive pancreatic cancer, which is the fourth and fifth leading cause of death in men and women, respectively, in developed countries.<sup>2</sup> In one study, about 75% of all

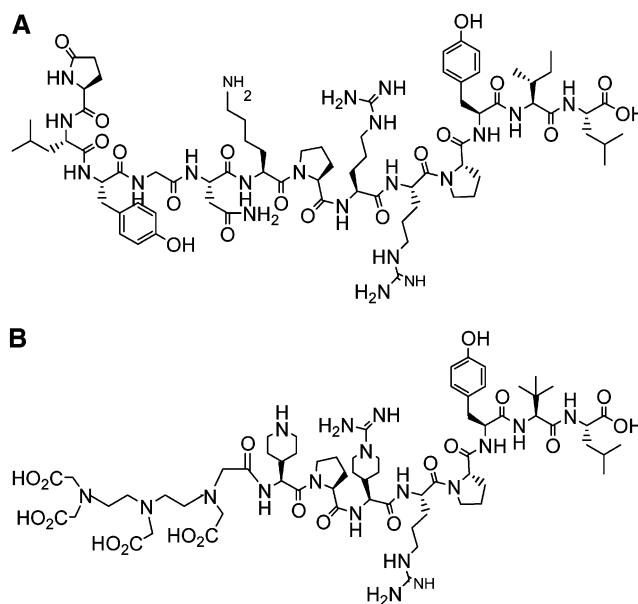


**Figure 1.** Structures of (A) neurotensin and (B) a representative stable and high neurotensin receptor binding DTPA neurotensin peptide analogue (17).

ductal pancreatic adenocarcinomas were NTR1-positive.<sup>5</sup> A recent report further suggests that, whereas the expression of NTR1 mRNA is increased in pancreatic cancer and chronic pancreatitis relative to normal pancreas, only pancreatic cancer cells translate the

\* Corresponding author. Phone: 314-362-8599; E-mail: achilefu@mir.wustl.edu.

<sup>†</sup> Mallinckrodt Institute of Radiology.

<sup>§</sup> Mallinckrodt Inc.

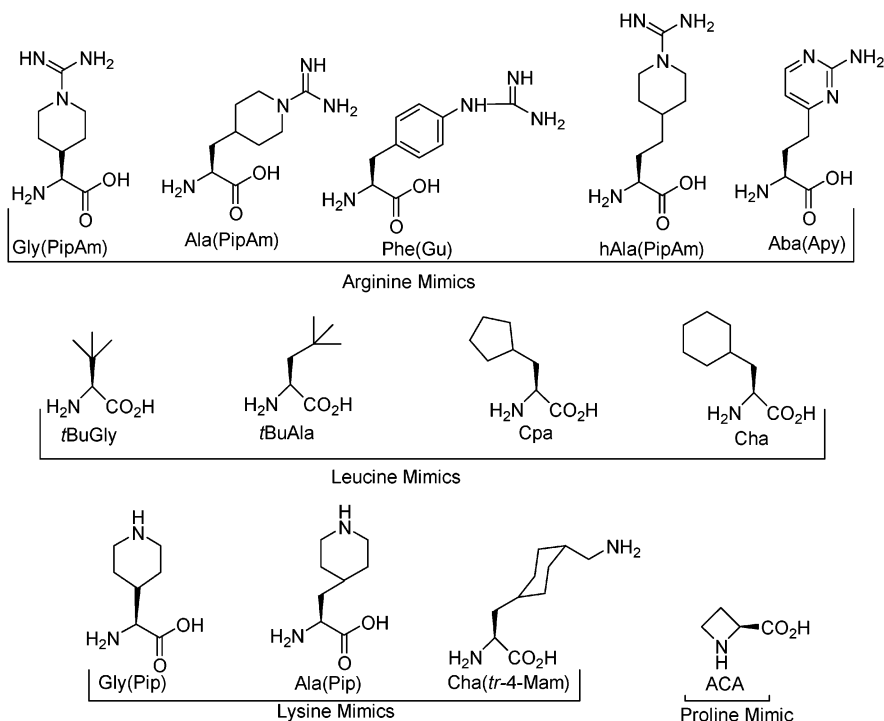


**Figure 2.** Structures and abbreviations of unusual amino acids used in this study. Abbreviations: Gly(PipAm), 4-piperidinyl-(*N*-amidino)-*S*-glycine; Ala(PipAm), 4-piperidinyl(*N*-amidino)-*L*-alanine; Phe(Gu), 4-guanidino-*L*-phenylalanine; hAla(PipAm), 4-piperidinyl(*N*-amidino)-*L*-homoalanine; Aba(Apy), 2-amino-4[(2-amino)pyrimidinyl]butanoic acid; tBuGly, *tert*-butyl-*S*-glycine; tBuAla, *tert*-butyl-*L*-alanine; Cpa, cyclopentyl-*L*-alanine; Cha, cyclohexyl-*L*-alanine; Gly(Pip), 4-piperidinyl-*S*-glycine; Ala(Pip), 4-piperidinyl-*L*-alanine; Cha(*tr*-4-Mam), *trans*-cyclohexyl(4-aminomethyl)-*L*-alanine; ACA, *L*-azetidine-2-carboxylic acid.

NTR1 mRNA into the protein receptor.<sup>6</sup> Thus, in addition to monitoring the expression of NTR in the pancreas, NTR-avid imaging agents can also distinguish pancreatic cancer from chronic pancreatitis and normal pancreas.

Unfortunately, native NT is not a suitable carrier for delivering NTR-specific imaging agents to tumors *in vivo* because of its short half-life (1.5 min) in human plasma.<sup>7</sup> Previous studies showed that a truncated NT analogue, NT(8–13), has a similar NTR binding affinity and a longer half-life (10 min) in plasma than NT but the peptide degrades rapidly before detectable quantities can selectively accumulate in NTR-positive tumors *in vivo*.<sup>7,8</sup> This instability is attributed to the rapid cleavage of the scissile Arg(8)-Arg(9) and Tyr(11)-Ile(12) amide bonds of NT by proteolytic enzymes.<sup>4,9</sup>

To circumvent this problem, numerous stabilization strategies have been reported, including the synthesis of non-peptide,<sup>10,11</sup> cyclic peptide,<sup>12</sup> and pseudo-NT peptide<sup>4,7,13,14</sup> analogues. Although the compounds have improved plasma stability, the synthetic challenge and generally low NTR binding affinity of the compounds relative to native NT limit their utility as a delivery vehicle for therapeutic drugs and imaging agents. These limitations can be overcome by using a simple synthetic approach to replace the metabolically active amino acid sequence with mimics that stabilize the entire molecule and retain high NTR binding affinity.<sup>15–18</sup>

On the basis of established NT degradation sites and the commercial availability of a variety of amino acid mimics that are amenable to automated Fmoc peptide synthesis strategy (Figure 1b), we prepared and systematically evaluated a series of NT peptide analogues and identified novel compounds that combine high NTR

binding affinity with high stability in biological media. Subsequent conjugation of metal chelators or fluorescent probes to the NT peptide analogues did not interfere with their NTR binding affinity, which remained in the low nanomolar range. Biodistribution studies show that <sup>111</sup>In-DTPA conjugates of the new NT peptide analogues preferentially accumulate in tumors relative to surrounding normal tissues. A combination of the ease of synthesis, exceptional stability in biological media, high NTR binding affinity, and adaptability to the presence of hydrophilic metal chelators or hydrophobic fluorescent probes provides a unique opportunity to use the compounds reported herein as tissue-specific diagnostic or cytotoxic drugs in the management of NTR-positive tumors.

## Results and Discussion

**Synthesis.** As a tridecapeptide, the synthesis of NT by standard Fmoc strategy is straightforward. Unfortunately, continuous infusion of NT would be needed to achieve a required biological effect *in vivo* because of its short half-life in plasma. Previous studies have shown that Arg(8)-Arg(9) and Tyr(11)-Ile(12) are the primary scissile amide bonds cleaved by proteolytic enzymes *in vivo*.<sup>9</sup> Consequently, we explored the use of commercially available lysine, arginine, and leucine mimics to stabilize the scissile amide bonds. Figure 2 shows the structures and abbreviations of the amino acid mimics used in this study. All of the amino acids are compatible with standard Fmoc peptide synthesis strategy<sup>19</sup> and were thus incorporated into the peptide backbone by automated solid-phase peptide synthesis. Consistent with our primary focus of developing tissue-specific imaging drugs, we incorporated a radiometal

**Table 1.** Structure, Receptor Binding Affinity, and Stability of Neurotensin Peptide Analogues<sup>a</sup>

no.	sequence	IC <sub>50</sub> (nM)	SE, ± (nM)	intact peptide (%) <sup>b</sup>	
				serum	urine
1	pGlu-Leu-Tyr-Glu-Asn-Lys-Pro-Arg-Arg-Pro-Tyr-Ile-Leu-OH (neurotensin) <sup>c</sup>	0.2	0.02	ND	ND
2	DTPA-Arg-Arg-Pro-Tyr-Ile-Leu-OH <sup>d</sup>	0.4	0.04	1.6	13.0
3	DTPA-DLys-Pro-Arg-Phe(4-Gu)-Pro-Tyr-Ile-leu-OH	0.4	0.06	16.3	0
4	DTPA-DLys-Pro-Phe(4Gu)-Arg-Pro-Tyr-Ile-leu-OH	0.5	0.05	14.1	1.5
5	DTPA-DLys-Pro-Aba(Apy)-Arg-Pro-Tyr-Ile-Leu-OH	10.2	3.30	4.3	6.0
6	DTPA-DLys-Pro-Phe(4-Gu)-Phe(4-Gu)-Pro-Tyr-Ile-Leu-OH	22.1	8.91	25.2	2.3
7	DTPA-DLys-Pro-Phe(4-Gu)-Arg-Pro-Tyr- <i>t</i> BuGly-Leu-OH	24.6	9.27	72.0	51.1
8	DTPA-DLys-Pro-Gly(PipAm)-Arg-Pro-Tyr- <i>t</i> BuGly-Leu-OH	0.4	0.06	87.5	63.0
9	DTPA-DLys-Pro-Gly(PipAm)-Arg-ACA-Tyr- <i>t</i> BuGly-Leu-OH	113	NA <sup>e</sup>	79.2	36.5
10	DTPA-DLys-Pro-Gly(PipAm)-Gly(Pip)-Pro-Tyr- <i>t</i> BuGly-Leu-OH	59.6	NA	91.6	79.7
11	DTPA-DLys-Pro-Gly(PipAm)-Arg-Pro-mTyr- <i>t</i> BuGly-Leu-OH	106	NA	84.4	57.8
12	DTPA-DLys-ACA-Gly(PipAm)-Arg-Pro-Tyr- <i>t</i> BuGly-Leu-OH	11.5	4.93	79.5	49.8
13	DTPA-Ala(Pip)-Pro-Gly(PipAm)-Arg-Pro-Tyr- <i>t</i> BuGly-Leu-OH	> 1000	NA	98.9	98.3
14	DTPA-DLys-Pro-Gly(PipAm)-Arg-Pro-DTyr- <i>t</i> BuGly-Leu-OH	0.6	0.12	98.9	98.3
15	DTPA-DLys-Pro-Ala(PipAm)-Arg-Pro-Tyr- <i>t</i> BuGly-Leu-OH	2.5	0.50	96.5	89.8
16	DTPA-DLys-Pro-hAla(PipAm)-Arg-Pro-Tyr- <i>t</i> BuGly-Leu-OH	6.3	1.83	84.3	71.3
17	DTPA-Gly(Pip)-Pro-Gly(PipAm)-Arg-Pro-Tyr- <i>t</i> BuGly-Leu-OH	0.3	0.03	95.9	93.6
18	DTPA-Cha( <i>tr</i> -4-Mam)-Pro-Gly(PipAm)-Arg-Pro-Tyr- <i>t</i> BuGly-Leu-OH	0.3	0.04	94.8	89.4
19	DTPA-DTyr-Glu-Asn-Lys-Pro-Gly(PipAm)-Arg-Pro-Tyr- <i>t</i> BuGly-Leu-OH	1.5	0.34	94.9	86.8
20	DTPA-DLys-Pro-Gly(PipAm)-Arg-Pro-Tyr- <i>t</i> BuGly-Cpa-OH	42.4	NA	88.1	73.6
21	DTPA-DLys-Pro-Gly(PipAm)-Arg-Pro-Tyr- <i>t</i> BuGly-Cha-OH	11.7	7.32	81.2	65.9
22	DTPA-DLys-Pro-Gly(PipAm)-Arg-Pro-Tyr- <i>t</i> BuGly- <i>t</i> BuAla-OH	21.7	4.47	89.2	72.3
23	DTPA-DTyr-Glu-Asn-Lys-Pro-Gly(PipAm)-Arg-Pro-Tyr- <i>t</i> BuGly-Cha-OH	0.6	0.02	93.9	81.8
24	DTPA-DTyr-Glu-Asn-Lys-Pro-Gly(PipAm)-Arg-Pro-Tyr- <i>t</i> BuGly- <i>t</i> BuAla-OH	0.4	0.09	98.9	89.8
25	α-FITC-DLys-Pro-Gly(PipAm)-Arg-Pro-Tyr-Ile-Leu-OH <sup>f</sup>	1.2	0.32	ND <sup>g</sup>	ND
26	ε-FITC-DLys-Pro-Gly(PipAm)-Arg-Pro-Tyr-Ile-Leu-OH	0.6	0.01	ND	ND
27	α,ε-Bis(FITC)-DLys-Pro-Gly(PipAm)-Arg-Pro-Tyr-Ile-Leu-OH	3.4	0.52	ND	ND
28	α-FITC-Gly(Pip)-Pro-Gly(PipAm)-Arg-Pro-Tyr- <i>t</i> BuGly-Leu-OH	0.5	0.09	ND	ND
29	Gly(FITC-Pip)-Pro-Gly(PipAm)-Arg-Pro-Tyr- <i>t</i> BuGly-Leu-OH	0.6	0.20	ND	ND
30	α-FITC-Gly(FITC-Pip)-Pro-Gly(PipAm)-Arg-Pro-Tyr- <i>t</i> BuGly-Leu-OH	2.6	0.60	ND	ND

<sup>a</sup> Abbreviations and structures of unusual amino acids are shown in Figure 2; IC<sub>50</sub> values were measured relative to <sup>111</sup>In-labeled **17**.

<sup>b</sup> Stability determined by analytical HPLC with a radiometric detector. <sup>c</sup> pGlu, pyroglutamic acid. <sup>d</sup> DTPA, diethylenetriaminepentaacetic acid on the α-amino group of N-terminal amino acid; DTPA was labeled with <sup>111</sup>InCl<sub>3</sub> for the stability study; only the tracer was labeled for NTR binding assay. <sup>e</sup> NA, not applicable because our assay was optimized for IC<sub>50</sub> values between 0.1 and 10 nM, values greater than 12 nM were obtained by extrapolating the data from a four parameter curve-fitting program. <sup>f</sup> FITC, fluorescein thiourea group. <sup>g</sup> ND, not determined.

chelator for nuclear imaging and fluorescein for optical imaging of NTR-positive tumors. In previous studies, we demonstrated that the DOTA and DTPA conjugates of bioactive peptides have similar IC<sub>50</sub> values for the target receptor.<sup>20</sup> On the basis of the facile synthesis of a reactive DTPA intermediate (tri-*tert*-butyl DTPA) that also eliminates the formation of bispeptide derivatives,<sup>21</sup> we used DTPA-NT peptide conjugates in this study. The tri-*tert*-butyl DTPA was conjugated to the N-terminus of NT peptide analogue on solid support by the same automated procedure used to assemble the peptide. TFA-mediated cleavage of the peptide from the resin and simultaneous removal of all side chain protecting groups yielded the desired products, which were purified by HPLC, lyophilized in MeCN/H<sub>2</sub>O, and characterized by LC-MS (Table 1, compounds **2–24**). The homogeneity of the compounds was established by using two diverse gradient HPLC conditions, as described in the Experimental Section.

Stability of the newly synthesized DTPA-NT peptide analogues in human serum and rat urine was evaluated by monitoring the HPLC spectral profile of each <sup>111</sup>In-DTPA-NT peptide analogue at 4 h postincubation (Figure 3). Radiolabeling of the DTPA-NT peptide analogues was accomplished by incubating the peptide with <sup>111</sup>InCl<sub>3</sub> at room temperature for 30 min. A small sample of the mixture (10 μCi) was analyzed by HPLC to determine the radiochemical purity (>95%) and radiolabeling yield (>99%).

To evaluate the potential of using these novel NT peptide analogues for optical imaging of tumors, we prepared their fluorescein (FITC) derivatives (Table 1, compounds **25–30**). Synthesis of the FITC derivatives was performed by solution-phase reaction because of previous observation that the resulting thiourea bond is unstable under TFA-mediated peptide cleavage from solid support.<sup>20</sup> Thus, reaction of fluorescein isothiocyanate with HPLC-purified NT peptide analogues yielded the desired compounds. The structural features of the two NT peptide analogues [NT(6–13)] used for FITC conjugation are predisposed to form different compounds under the solution-phase reaction conditions used. For example, the presence of lysine at the N-terminus of **25–27** [Lys(6)] gives two isomeric α- and ε-FITC derivatives and an additional α,ε-bis FITC conjugate. To prepare an authentic sample of each isomer, we used orthogonal groups to protect either the α- or the ε-amino group of Lys(6). Thus, an authentic sample of **25** was synthesized by using an α-fluorenylmethoxycarbonyl (Fmoc)-ε-1-(4,4-Dimethyl-2,6-dioxocyclohex-1-ylidene)-3-methylbutyl (Dde) protected lysine [Fmoc-Lys(Dde)-OH] at the N-terminus. After completing the peptide synthesis and deblocking the orthogonal protecting Fmoc group, the peptide was cleaved from the resin with TFA, which also removed all other amino acid side chain protecting groups except Dde. Subsequent reaction of the peptide with FITC and removal of the Dde with hydrazine gave exclusively the α-FITC compound **25**.

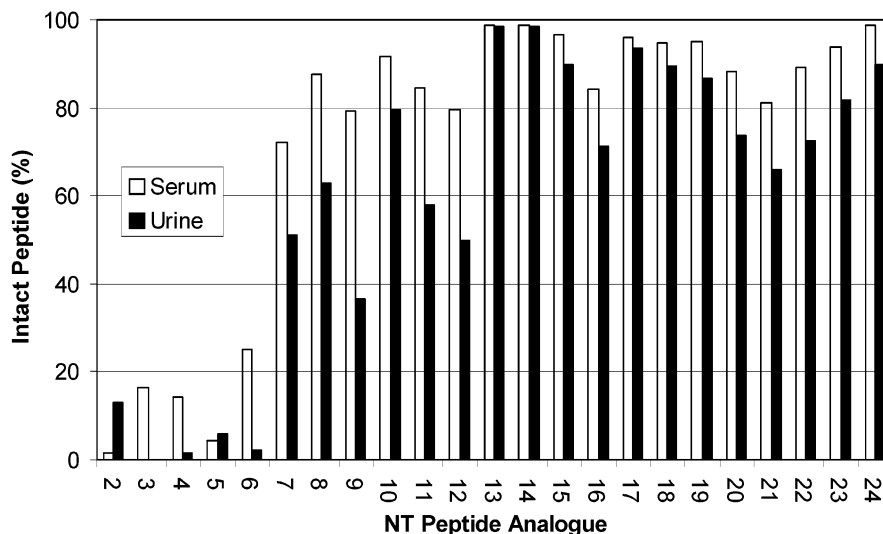


**Figure 3.** Stability of NT peptide analogues in human serum and rat urine determined by monitoring their HPLC spectral profile at 37 °C and 24 h postincubation.

A similar procedure was used to prepare an authentic sample of  $\epsilon$ -FITC analogue (**26**) by using Dde-Lys(Fmoc)-OH at the N-terminus.

Synthesis of the bis(FITC)-NT conjugate (**27**) was achieved by using Fmoc-Lys(Fmoc)-OH at the N-terminus, resulting in the liberation of two amino groups after removing the Fmoc with 20% piperidine in dimethylformamide (DMF). Cleavage of the peptide from the resin and subsequent reaction of the free  $\alpha,\epsilon$ -amino groups of Lys(6) with excess FITC gave **27**. We observed that nearly equimolar mixture of all three compounds (**25–27**) was obtained when the reaction was carried out with a 3:1 molar mixture of FITC and NT peptide analogue, respectively. The ease of separating **25–27** by HPLC facilitates their synthesis by the one-pot procedure described above. The identity of each isolated compound was confirmed by spiking a small HPLC sample of the conjugate with an authentic compound.

A similar strategy described above was used to prepare compounds **28–30**, which are obtained by reacting the corresponding peptide with FITC. In this case, Fmoc-Gly(PipBoc)-OH was used at the N-terminus. Authentic **29** was prepared by cleaving the peptide from solid support without removing the N-terminal Fmoc group. This strategy enables selective reaction of FITC with the piperidine amino group of Gly(Pip), followed by removing the Fmoc protecting group with 20% piperidine in DMF. Simultaneous preparation of all three compounds **28–30** was accomplished by a similar one-pot procedure described above. The bis-FITC conjugate (**30**) was readily identified by mass spectrometry (MS), and the isomeric compounds **28** and **29** were identified by spiking the HPLC sample with authentic **29**.

The absorption and fluorescence emission of FITC-NT peptide analogues were performed in 25% aqueous DMSO at low concentrations ( $<1 \mu\text{M}$ ), and the spectral profile of all the FITC peptide conjugates were similar. Typically, two peaks centered at about 460 nm and 480 nm in the absorption spectra and a broad peak at 520 nm (excitation wavelength 480 nm) were observed in the emission spectra.

Unlike many published stabilization strategies, the NT peptide analogues described above were prepared by standard automated peptide synthesis procedure, without the need for extensive postsynthetic modifications. In fact, the DTPA conjugation was also achieved without additional user intervention. With the availability of numerous amino acid mimics from commercial sources, our approach should make it easier to prepare a combinatorial library of stable NT peptide analogues with high NTR binding affinity.

**Stability Studies.** Attempts to use NT or its truncated peptide analogue, NT(8–13) for in vivo imaging and metabolism studies<sup>8,22,23</sup> by labeling them with diagnostic radionuclides were not successful because of the inherent instability of these compounds in vivo. Consequently, we evaluated the stability of the new NT peptide analogues in human serum and rat urine (Figure 3). To minimize a possible interaction of negatively charged DTPA carboxylates with the positively charged Arg(8) guanidino group at physiological pH, which may reduce metal chelate stability and possibly interfere with NTR binding affinity in vivo,<sup>4,7,9</sup> we used NT(6–13) peptide analogues as the basic structural framework for most of the new compounds prepared. In general, the resulting N-terminal Lys(6) was replaced with the metabolically stable D-isomer or other lysine mimics.

The DTPA-NT peptide analogues were radiolabeled with <sup>111</sup>In to monitor their stability profile by an HPLC system equipped with a radiometric and a UV detector. Formation of metabolites is typically indicated by the appearance of peaks with shorter retention times. All stability studies were performed at 4 h postincubation at 37 °C. Starting with NT(6–13) as template, we replaced either Arg(8) or Arg(9) with arginine mimics (compounds **3–5**), but these substitutions did not improve the stability of the resulting compounds in either serum or urine. Further replacement of both Arg(8)-Arg(9) with mimics (compound **6**) had little effect on the in vivo stability of the NT peptide analogue. These results suggest that enzymatic cleavage at other scissile amide bonds contributes to the degradation of NT peptide

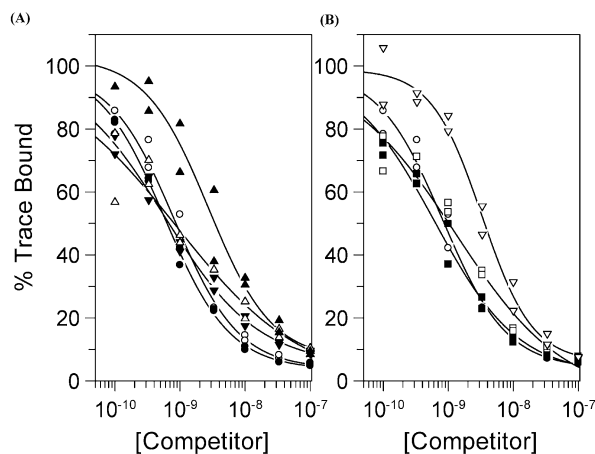


**Figure 4.** Representative inhibition of [ $^{111}\text{In}$ ]-DTPA-neurotensin peptide analogue (**17**) binding to HT29 membranes using varying concentrations of the neurotensin analogues listed in Table 1. Symbols corresponding to analogue numbers given in Table 1 are (A)  $\circ$ , **8**;  $\bullet$ , **1**;  $\square$ , **25**;  $\blacksquare$ , **26**;  $\nabla$ , **27**; and (B)  $\circ$ , **8**;  $\blacktriangledown$ , **28**;  $\blacktriangle$ , **29**;  $\nabla$ , **30**.

analogues in vivo, an observation that supports previous reports that Tyr(11)-Ile(12) amide bond is particularly susceptible to cleavage by proteolytic enzymes.<sup>9,24</sup>

To address this additional source of instability, we incorporated leucine mimics at the C-terminus of NT(6–13) while retaining previously inserted arginine mimics. As shown in Table 1 and Figure 3, replacement of Ile(12) with *tert*-butyl glycine dramatically improved the metabolic stability of the NT peptide analogues in serum and urine (**7–19**). Subsequent replacement of both Ile(12) and Leu(13) with mimics (**20–24**) did not improve the stability further, suggesting that cleavage of the Ile(12)-Leu(13) amide bond may play a minor role in NT degradation. Although Pro(10)-Tyr(11) amide bond is reported to be cleaved by two endopeptidases,<sup>9</sup> replacement of Pro(10) with a proline mimic (ACA, compound **9**) did not further enhance peptide's stability beyond that provided by *t*BuGly. However, substitution of Tyr(11) with the D-isomer (compound **14**) conferred greater stability on the molecule than nearly all of the NT peptide analogues prepared. Hence, a stabilization strategy may also involve subtle changes at the Tyr(11) position and suggests that the NT amide bond most susceptible to degradation is the Tyr(11)-Ile(12) sequence. These results demonstrate that selective substitution of amino acid mimics at the scissile amide bonds stabilized the DTPA-NT peptide analogues in biological media. The in vitro stability of compounds **25–30** were not evaluated.

**NTR Binding Affinity.** In addition to enhancing the metabolic stability of NT, we were also interested in preparing NT peptide analogues that have high NTR binding affinity. Determination of the  $\text{IC}_{50}$  values of putative bioactive molecules is an effective and a rapid approach to assess their bioactivity. Accordingly, we performed the competitive binding assays of all new NT peptide analogues prepared by using [ $^{111}\text{In}$ ]-DTPA-NT peptide analogue (**17**, Figure 1b) as tracer and reference. Representative  $\text{IC}_{50}$  curves are shown in Figure 4. The established human adenocarcinoma cell line (HT29) tumor model was used for both in vitro and in vivo studies because it expresses NTR1 that is prevalent in human pancreatic cancers.<sup>6</sup> It should be noted that our

NTR binding assays consistently gave lower  $\text{IC}_{50}$  values than those reported in the literature for NT (**1**) and the truncated peptide analogue **2**,<sup>4,9</sup> but a similar trend was obtained at all times. Our results show that substitution of either Arg(8) or Arg(9) with Phe(4-Gu) arginine mimic (compounds **3** and **4**) retained the high NTR binding affinity of NT. However, the NTR binding affinity decreased considerably when two Phe(4-Gu), or Gly-(PipAM) and Gly(Pip), replaced both Arg(8) and Arg(9) (compounds **6** and **10**), probably due to steric effects in fitting two bulky and less flexible phenyl or piperidiny guanidino groups into the NTR binding site. Consequently, we replaced only Arg(8) with mimics in subsequent NT peptide derivatives because this is a primary cleavage site of NT and its natural amino acid-based peptide analogues.

Modification of the amino acids at the C-terminal portion of NT(6–13) affected its NTR binding affinity. We observed that replacing Ile(12) with *t*BuGly stabilized the peptide and generally resulted in compounds that possess high NTR binding affinity. However, modifications at the Pro(10) and Tyr(11) regions of NT(6–13) reduced the receptor binding affinity of the resulting peptides (compounds **9** and **11**). In general, attempts to replace both Ile(12) and Leu(13) in NT(6–13) with leucine mimics reduced the NTR binding affinity (**20–22**), but this affinity was reestablished when additional amino acids were incorporated at the N-terminus (**23** and **24**). The exact reason for this observation is not clear at this point.

Interestingly, conjugation of FITC to the N-terminus of the new bioactive NT peptide analogues did not perturb their NTR binding affinity (**25–30**), as was seen with some of the DTPA conjugates. All of the FITC derivatives had high receptor binding affinity and incorporation of two fluorescein moieties per NT peptide analogue was not deleterious to the NTR binding affinity. These observations show that the FITC-NT-peptide conjugates can be used as NTR-specific molecular beacons for optical imaging of NTR-positive tumors. Thus, conjugation of molecular probes and possibly therapeutic drugs at Lys(6) or its mimics does not compromise the NTR binding affinity of the ensuing NT peptide analogues.

**Biodistribution Studies.** Because of the exceptional metabolic stability in biological media and the high NTR binding affinity of compound **17** (Figure 1b), we evaluated its biodistribution in NTR-positive HT29 tumor-bearing SCID mice. The HT29 cells were harvested, and about  $1 \times 10^6$  cells were injected subcutaneously into the bilateral flank of SCID mice. After the tumor had grown to about 0.3 g, the mice were injected with [ $^{111}\text{In}$ ]-In-labeled DTPA-NT (**17**), followed by necropsy of each group of three mice at 1 and 4 h postinjection. Radioassay was performed on major organs, as shown in Figure 5. Apart from the kidneys, which are the primary route of excretion, compound **17** was selectively taken up by the NTR-positive tumor tissue. At 1 h postinjection, uptake of the radiolabeled **17** in the tumor (2.83% ID/g) and the kidneys (6.14% ID/g) were observed, while its accumulation in other organs was negligible (Table 2). The clearance of **17** from blood was rapid within 1 h postinjection (0.4% ID/g) and the uptake in the kidneys and tumor tissues slightly reduced to 5.6% and 2.6%

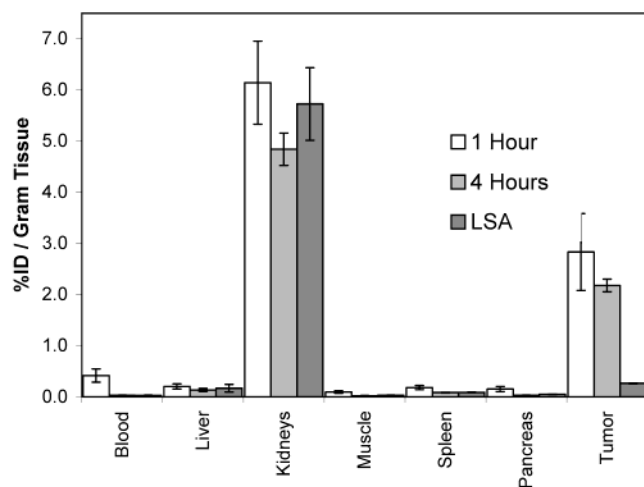


**Figure 5.** Biodistribution of [In-111]-NT peptide analogue (**17**) in HT29 tumor-bearing SCID mice at 3 h postinjection and graphed as % injected dose per gram tissue; LSA, low specific activity (0.5 Ci/mmol) radiolabeled NT-peptide used to demonstrate NT receptor specific uptake.

**Table 2.** Biodistribution of  $^{111}\text{In}$ -DTPA-NT Peptide Analogue **17** in HT29 Tumor Implanted SCID Mice (%ID/g tissue  $\pm$  SE,  $n = 3$ )

tissue sample	1 h	4 h	LSA <sup>a</sup>
blood	0.416 $\pm$ 0.130	0.030 $\pm$ 0.004	0.027 $\pm$ 0.006
liver	0.203 $\pm$ 0.051	0.133 $\pm$ 0.028	0.168 $\pm$ 0.074
kidneys	6.141 $\pm$ 0.812	4.841 $\pm$ 0.315	5.725 $\pm$ 0.710
muscle	0.092 $\pm$ 0.024	0.021 $\pm$ 0.002	0.030 $\pm$ 0.002
spleen	0.180 $\pm$ 0.040	0.085 $\pm$ 0.007	0.088 $\pm$ 0.005
pancreas	0.152 $\pm$ 0.049	0.030 $\pm$ 0.002	0.051 $\pm$ 0.004
tumor	2.831 $\pm$ 0.751	2.177 $\pm$ 0.123	0.263 $\pm$ 0.011

<sup>a</sup> LSA, low specific activity (0.5 Ci/mmol) radiolabeled NT-peptide used to demonstrate NT receptor specific uptake.

ID/g, respectively, at 4 h postinjection, when the compound was barely detectable in all other organs. Blocking studies (low specific activity; LSA) showed that at 4 h postinjection, retention of radiolabeled **17** in the NTR-positive tumor tissue was inhibited by cold (non-radioactive) NT, confirming that its uptake is NTR-mediated. In contrast, the kidney uptake of **17** was not affected by the blocking study. In fact, a slight increase in kidney uptake was observed at 4 h post LSA administration relative to the unblocked study, suggesting that blocking the NTR-positive tumor uptake of the radiolabeled peptide accounted for the additional kidney uptake of the compound by a nonspecific mechanism.

## Conclusion

As shown in Table 1, we successfully prepared a library of NT peptide analogues with different degrees of stability and NTR binding affinity. However, high metabolic stability in biological media did not necessarily translate into high NTR binding affinity. We found that the best combination of high NTR binding affinity and metabolic stability was obtained when Lys(6), Arg(8), and Ile(12) were substituted with the appropriate amino acid mimics and using NT(6–13) as template. Additional stability was obtained by substituting Tyr(11) with the D-isomer. In vivo biodistribution studies showed that the selective uptake of **17** in NTR-positive tumor-bearing SCID mice is NTR-specific. Therefore, the structural feature of **17** can be exploited

to selectively deliver diagnostic and therapeutic drugs to target tissues, which minimizes the deleterious effects of toxic drugs on healthy tissues.

## Materials and Methods

**General.** All reagents and solvents were obtained commercially and used without further purification. Amino acids were purchased from RSP Amino Acid Analogues, Inc., Hopkinton, MA. Native NT was purchased from commercial sources. The amino acids are all compatible with standard Fmoc peptide synthesis procedure on solid support, and they are in the L-configuration, unless otherwise stated. Purification and analysis of the new NT peptide analogues were performed on an HPLC system equipped with a tunable UV-visible detector. Analytical (flow rate = 0.5 mL/min) and semi-preparative (flow rate = 10 mL/min) RP-HPLC were performed as described in the literature by using a C-18 column.<sup>25</sup> The gradient elution protocol ranged from a mixture of 95% A and 5% B to 30% A and 70% B in 30 min, where A is 5% MeCN/0.1% aqueous TFA and B is 90% MeCN/0.1% TFA in 9.9% HPLC grade water. All percentages are expressed in v/v. A second elution system consisting of an isocratic mixture of 60% H<sub>2</sub>O containing 0.1% TFA, 30% MeOH, and 10% MeCN was used to confirm the homogeneity of the compounds by analytical HPLC. Peak detection was at 214 nm, unless otherwise stated. Electrospray ionization mass spectrometry (EI-MS) experiments were performed on a triple quadrupole mass spectrometer. The electrospray interface was operated in positive ion mode with a spray voltage of 4.5 kV and a capillary temperature of 225 °C. Samples were introduced into the spectrometer by flow injection utilizing 70% MeCN and 30% H<sub>2</sub>O containing 0.1% TFA. The absorption and emission spectra of the fluorescein conjugates were performed on a Cary 500 UV-visible spectrophotometer (Varian) and QuantaMaster spectrofluorometer (Photon Technology International), respectively. The HPLC purity of all compounds used in the in vivo and in vitro studies was >99%.

**Synthesis of DTPA-NT Peptide Analogues 2–24.** All of the peptides were prepared as described below and exceptions are noted under specific peptides. The peptides were synthesized on solid support by standard automated Fmoc procedures.<sup>19</sup> Commercially preloaded leucine resin was used for preparing most of the peptides at a 25  $\mu\text{mol}$  scale. For all other peptides with carboxyl terminal amino acids other than leucine, the amino acid was loaded on a Wang resin at a substitution of about 0.6 mmol/g of resin by standard CsI-mediated esterification. Automated activation of the carboxyl group of Fmoc-protected amino acids (75  $\mu\text{mol}$ ) with a 1:1 mixture of *N*-hydroxybenzotriazole (HOBt, 2 M) and 2-(1-H benzotriazol-1-yl)-1,1,1,3-tetramethyluronium hexafluorophosphate (HBTU, 2 M) and subsequent coupling to resin-bound amino acids was used to assemble the peptide. Coupling of DTPA was accomplished by placing tri-*tert*-butyl DTPA (75  $\mu\text{mol}$ ) in the last cartridge of peptide synthesizer's amino acid rack, which was then coupled to the N-terminus by the same automated method used to assemble the peptide.<sup>21</sup> Fmoc was removed at the end of each coupling cycle with 20% piperidine in DMF and anhydrous tetrahydrofuran (THF) was used to wash the resin at the completion of peptide synthesis. Cleavage of the peptides from the resin and concomitant removal of the side-chain protecting groups were accomplished with 85% TFA, 5% H<sub>2</sub>O, 5% PhOH, and 5% thioanisole for 4 h at room temperature. The crude peptides were precipitated with cold *tert*-butyl methyl ether and purified by RP-HPLC using gradient elution protocol described in the general section above. All of the peptides and their conjugates were characterized by analytical HPLC and electrospray MS (EI-MS) analysis after lyophilization in 67% H<sub>2</sub>O and 33% MeCN.

**DTPA-Arg-Arg-Pro-Tyr-Ile-Leu-OH (2):** EI-MS  $m/z$  1193 [M + H]<sup>+</sup>, 597 [M + 2H]<sup>2+</sup>, 398 [M + 3H]<sup>3+</sup>.

**DTPA-DLys-Pro-Arg-Phe(4-Gu)-Pro-Tyr-Ile-leu-OH (3):** EI-MS  $m/z$  1466 [M + H]<sup>+</sup>, 734 [M + 2H]<sup>2+</sup>, 489 [M + 3H]<sup>3+</sup>.

**DTPA-DLys-Pro-Phe(4Gu)-Arg-Pro-Tyr-Ile-leu-OH (4):** EI-MS  $m/z$  1465 [M + H]<sup>+</sup>, 734 [M + 2H]<sup>2+</sup>, 489 [M + 3H]<sup>3+</sup>.

**DTPA-DLys-Pro-Aba(Apy)-Arg-Pro-Tyr-Ile-Leu-OH (5):** EI-MS  $m/z$  1440 [M + H]<sup>+</sup>, 721 [M + 2H]<sup>2+</sup>, 489 [M + 3H]<sup>3+</sup>.

**DTPA-DLys-Pro-Phe(4-Gu)-Phe(4-Gu)-Pro-Tyr-Ile-Leu-OH (6):** EI-MS  $m/z$  1514 [M + H]<sup>+</sup>, 758 [M + 2H]<sup>2+</sup>, 506 [M + 3H]<sup>3+</sup>.

**DTPA-DLys-Pro-Phe(4-Gu)-Arg-Pro-Tyr-tBuGly-Leu-OH (7):** EI-MS  $m/z$  1465 [M + H]<sup>+</sup>, 733 [M + 2H]<sup>2+</sup>, 489 [M + 3H]<sup>3+</sup>.

**DTPA-DLys-Pro-Gly(PipAm)-Arg-Pro-Tyr-tBuGly-Leu-OH (8):** EI-MS  $m/z$  1444 [M + H]<sup>+</sup>, 723 [M + 2H]<sup>2+</sup>, 482 [M + 3H]<sup>3+</sup>.

**DTPA-DLys-Pro-Gly(PipAm)-Arg-ACA-Tyr-tBuGly-Leu-OH (9):** EI-MS  $m/z$  1430 [M + H]<sup>+</sup>, 716 [M + 2H]<sup>2+</sup>, 477 [M + 3H]<sup>3+</sup>.

**DTPA-DLys-Pro-Gly(PipAm)-Gly(Pip)-Pro-Tyr-tBuGly-Leu-OH (10):** EI-MS  $m/z$  1429 [M + H]<sup>+</sup>, 715 [M + 2H]<sup>2+</sup>, 477 [M + 3H]<sup>3+</sup>.

**DTPA-DLys-Pro-Gly(PipAm)-Arg-Pro-mTyr-tBuGly-Leu-OH (11):** EI-MS  $m/z$  1444 [M + H]<sup>+</sup>, 723 [M + 2H]<sup>2+</sup>, 482 [M + 3H]<sup>3+</sup>.

**DTPA-DLys-ACA-Gly(PipAm)-Arg-Pro-Tyr-tBuGly-Leu-OH (12):** EI-MS  $m/z$  1430 [M + H]<sup>+</sup>, 716 [M + 2H]<sup>2+</sup>, 477 [M + 3H]<sup>3+</sup>.

**DTPA-Ala(Pip)-Pro-Gly(PipAm)-Arg-Pro-Tyr-tBuGly-Leu-OH (13):** EI-MS  $m/z$  1471 [M + H]<sup>+</sup>, 736 [M + 2H]<sup>2+</sup>, 491 [M + 3H]<sup>3+</sup>.

**DTPA-DLys-Pro-Gly(PipAm)-Arg-Pro-DTyr-tBuGly-Leu-OH (14):** EI-MS  $m/z$  1444 [M + H]<sup>+</sup>, 723 [M + 2H]<sup>2+</sup>, 482 [M + 3H]<sup>3+</sup>.

**DTPA-DLys-Pro-Ala(PipAm)-Arg-Pro-Tyr-tBuGly-Leu-OH (15):** EI-MS  $m/z$  1458 [M + H]<sup>+</sup>, 730 [M + 2H]<sup>2+</sup>, 487 [M + 3H]<sup>3+</sup>.

**DTPA-DLys-Pro-hAla(PipAm)-Arg-Pro-Tyr-tBuGly-Leu-OH (16):** EI-MS  $m/z$  1472 [M + H]<sup>+</sup>, 737 [M + 2H]<sup>2+</sup>, 491 [M + 3H]<sup>3+</sup>.

**DTPA-Gly(Pip)-Pro-Gly(PipAm)-Arg-Pro-Tyr-tBuGly-Leu-OH (17):** EI-MS  $m/z$  1455 [M + H]<sup>+</sup>, 729 [M + 2H]<sup>2+</sup>, 486 [M + 3H]<sup>3+</sup>.

**DTPA-Cha(tr-(4-Mam)-Pro-Gly(PipAm)-Arg-Pro-Tyr-tBuGly-Leu-OH (18):** EI-MS  $m/z$  1498 [M + H]<sup>+</sup>, 750 [M + 2H]<sup>2+</sup>, 500 [M + 3H]<sup>3+</sup>.

**DTPA-DTyr-Glu-Asn-Lys-Pro-Gly(PipAm)-Arg-Pro-Tyr-tBuGly-Leu-OH (19):** EI-MS  $m/z$  1851 [M + H]<sup>+</sup>, 926 [M + 2H]<sup>2+</sup>, 617 [M + 3H]<sup>3+</sup>, 463 [M + 4H]<sup>4+</sup>.

**DTPA-DLys-Pro-Gly(PipAm)-Arg-Pro-Tyr-tBuGly-Cpa-OH (20):** EI-MS  $m/z$  1442 [M + H]<sup>+</sup>, 722 [M + 2H]<sup>2+</sup>, 481 [M + 3H]<sup>3+</sup>.

**DTPA-DLys-Pro-Gly(PipAm)-Arg-Pro-Tyr-tBuGly-Cha-OH (21):** EI-MS  $m/z$  1484 [M + H]<sup>+</sup>, 743 [M + 2H]<sup>2+</sup>, 495 [M + 3H]<sup>3+</sup>.

**DTPA-DLys-Pro-Gly(PipAm)-Arg-Pro-Tyr-tBuGly-tBuAla-OH (22):** EI-MS  $m/z$  1458 [M + H]<sup>+</sup>, 730 [M + 2H]<sup>2+</sup>, 487 [M + 3H]<sup>3+</sup>.

**DTPA-DTyr-Glu-Asn-Lys-Pro-Gly(PipAm)-Arg-Pro-Tyr-tBuGly-Cha-OH (23):** EI-MS  $m/z$  1890 [M + H]<sup>+</sup>, 946 [M + 2H]<sup>2+</sup>, 631 [M + 3H]<sup>3+</sup>, 473 [M + 4H]<sup>4+</sup>.

**DTPA-DTyr-Glu-Asn-Lys-Pro-Gly(PipAm)-Arg-Pro-Tyr-tBuGly-tBuAla-OH (24):** EI-MS  $m/z$  1864 [M + H]<sup>+</sup>, 933 [M + 2H]<sup>2+</sup>, 622 [M + 3H]<sup>3+</sup>, 467 [M + 4H]<sup>4+</sup>.

**One-Pot Procedure for the Synthesis of FITC-NT Peptide Analogues (25–30).** The FITC-NT peptide conjugates were prepared as described previously.<sup>20</sup> Briefly, the peptide was first synthesized by standard Fmoc procedure, and the N-terminal Fmoc protecting group was removed with 20% piperidine in DMF. Cleavage of the peptides from the resin and concomitant removal of the side-chain protecting groups were accomplished with 85% TFA, 5% H<sub>2</sub>O, 5% PhOH, and 5% thioanisole for 4 h at room temperature. The crude peptides were precipitated with cold MTBE and analyzed by RP-HPLC using gradient elution protocol described in the general section

above. The peptides are typically used for conjugating FITC without further purification, unless the analytical HPLC spectrum indicates the presence of impurities >15%. In these situations, the crude peptide was purified by semipreparative HPLC, as described in the general section above, before FITC conjugation reaction. The two peptides used to prepare the FITC conjugates have two reactive amino groups that allows for the preparation of all three FITC conjugates per peptide residue in a single reaction.

To synthesize compounds **25–27**, the peptide Gly(Pip)-Pro-Gly(PipAm)-Arg-Pro-Tyr-Gly-Lys-OH (12 mg, 11  $\mu$ mol), FITC (12 mg, 28  $\mu$ mol), and NaHCO<sub>3</sub> (10 mg, 120  $\mu$ mol) in DMF (1 mL) were stirred for 16 h at room temperature. The mixture was filtered into cold MTBE (8 mL) to give a yellow-orange precipitate. The supernatant was removed after centrifugation, and the crude product was washed with MTBE (3  $\times$  3 mL), dried under vacuum, and lyophilized in a mixture of MeCN/H<sub>2</sub>O. Analytical HPLC of the crude product showed three distinct peaks, which were isolated by semipreparative HPLC. Differentiation of the bis- (**27**) from the isomeric  $\alpha$ - (**25**) and  $\epsilon$ - (**26**) FITC conjugates was accomplished by mass spectral analysis. Because the isomeric compounds have the same molecular weight, their identity was confirmed by spiking a HPLC sample of each isolated fraction with the authentic compound, which was prepared as described below. The yield of each isolated compound ranged from 10 to 15%, based on the amount of peptide used. A similar one-pot synthesis procedure was used to prepare compounds **28–30**.

**Synthesis of Authentic Samples of Isomeric  $\alpha$ - and  $\epsilon$ -FITC NT Peptide Analogues 25 and 26.** The peptides were prepared as described above, except that Fmoc-Lys(Dde)-OH and Dde-Lys(Fmoc)-OH were used at the N-terminus to prepare the  $\alpha$ - and  $\epsilon$ -FITC conjugates, respectively. The N-terminal Fmoc protecting group was removed before cleavage of the peptide from the resin. Because the cleavage protocol leaves the Dde intact, FITC selectively reacts with the free amino group that was protected with Fmoc. The resulting crude FITC-labeled peptide was dissolved in a solution of 2% hydrazine in DMF (1 mL) and allowed to stand at room temperature for 20 min in order to remove the ivDde. The desired compound was obtained by precipitating the reaction mixture in cold MTBE, followed by lyophilization in MeCN/H<sub>2</sub>O and subsequent purification by semipreparative HPLC. The overall yield relative to the initial amount of peptide used in the reaction was about 40%.

**Synthesis of Authentic Samples of FITC NT Peptide Analogue 29.** A similar method described above was used to obtain the authentic samples of the isomers, except that the N-terminal Fmoc protecting group was not removed prior to cleavage of the peptide from the resin. This allowed FITC to selectively react with the piperidinyl amino group. After the FITC conjugation was complete, the Fmoc was removed with 20% piperidine in DMF, and workup was performed as described above.

**$\alpha$ -FITC-DLys-Pro-Gly(PipAm)-Arg-Pro-Tyr-Ile-Leu-OH (25):** EI-MS  $m/z$  1458 [M + H]<sup>+</sup>, 729 [M + 2H]<sup>2+</sup>, 487 [M + 3H]<sup>3+</sup>.

**$\epsilon$ -FITC-DLys-Pro-Gly(PipAm)-Arg-Pro-Tyr-Ile-Leu-OH (26):** EI-MS  $m/z$  1458 [M + H]<sup>+</sup>, 730 [M + 2H]<sup>2+</sup>, 487 [M + 3H]<sup>3+</sup>, 365 [M + 4H]<sup>4+</sup>.

**$\alpha,\epsilon$ -Bis(FITC)-DLys-Pro-Gly(PipAm)-Arg-Pro-Tyr-Ile-Leu-OH (27):** EI-MS  $m/z$  1847 [M + H]<sup>+</sup>, 924 [M + 2H]<sup>2+</sup>, 617 [M + 3H]<sup>3+</sup>.

**$\alpha$ -FITC-Gly(Pip)-Pro-Gly(PipAm)-Arg-Pro-Tyr-tBuGly-Leu-OH (28):** EI-MS  $m/z$  1470 [M + H]<sup>+</sup>, 736 [M + 2H]<sup>2+</sup>, 491 [M + 3H]<sup>3+</sup>.

**Gly(FITC-Pip)-Pro-Gly(PipAm)-Arg-Pro-Tyr-tBuGly-Leu-OH (29):** EI-MS  $m/z$  1469 [M + H]<sup>+</sup>, 736 [M + 2H]<sup>2+</sup>, 491 [M + 3H]<sup>3+</sup>.

**$\alpha$ -FITC-Gly(FITC-Pip)-Pro-Gly(PipAm)-Arg-Pro-Tyr-tBuGly-Leu-OH (30):** EI-MS  $m/z$  1847 [M + H]<sup>+</sup>, 930 [M + 2H]<sup>2+</sup>, 620 [M + 3H]<sup>3+</sup>, 466 [M + 4H]<sup>4+</sup>.

**In Vitro Receptor Binding Assays.** Receptor binding assays were performed by using membranes prepared from

the human adenocarcinoma cell line HT29. Membranes were prepared by a method similar to that previously reported.<sup>26</sup> Assays were carried out using Millipore Duroper membrane 96-well plates and the Millipore Multiscreen system, (Bedford, MA). Membrane plates were blocked with buffer (50 mM Tris-HCl pH 7.4, 5 mM MgCl<sub>2</sub>, 1 mg/mL BSA) for 2 h prior to use. The competitive receptor binding of the tracer <sup>111</sup>In-DTPA-NT peptide analogue **17** to HT29 cell membranes (50 μg/well) was determined in the presence of increasing concentration of cold competitors in buffer (50 mM Tris-HCl pH 7.4, 5 mM MgCl<sub>2</sub>, 1.0 mg/mL BSA) in a total volume of 200 μL per well. Following incubation for 90 min at room temperature, membranes were filtered by centrifugation at 1500g and washed with 150 μL buffer. The filters containing membrane bound radioactivity were removed from the assay plate and counted using a Packard Cobra gamma counter (Meriden, CT). IC<sub>50</sub> values were calculated using a four-parameter curve fitting routine using the program GraFit (Erithacus Software, UK). Radiolabeling of DTPA-linked peptides was carried out in 25 mM NaOAc, 12.5 mM sodium ascorbate (pH 4.5, room temperature, 30 min incubation). The specific activity of radiolabeled peptides was >1500 Ci/mmol. Radiochemical yield (>99.5%) and radiochemical purity (>98%) were determined by reverse phase chromatography on a C18 Vydac column using a MeCN/0.1% TFA gradient (5% to 70% MeCN over 20 min) at a flow rate of 1 mL/min. Binding assays were performed in triplicates per sample, and the experiments were repeated twice. The stock solutions of FITC-labeled peptides were prepared by adding an accurate amount of the weighed bioconjugate to 25% DMSO in water, and other concentrations were obtained by serial dilution of aliquots from the stock.

**Stability in Human Serum and Rat Urine.** The serum stability of <sup>111</sup>In-labeled NT analogues was evaluated by incubation in human serum (50% serum:50% PBS) at 37 °C for 4 h. The percent intact peptide after incubation was determined by separating degradation products by reverse phase HPLC using a Vydac C-18 column equipped with a radiometric and a UV detector and using a 15 min, 0 to 70% linear acetonitrile gradient (0.1% TFA/water). A similar procedure was used to determine the stability of radiolabeled peptides in rat urine (50% urine:50% PBS). Rat urine was collected from male Lewis rats and stored at -80 °C until use. After incubation at 37 °C for 4 h, <sup>111</sup>In-labeled NT analogues were chromatographed as described above. No significant change in the HPLC trace of any of the <sup>111</sup>In-labeled NT analogues was observed in control incubation in PBS alone for 4 h at 37 °C, and greater than 95% of the intact <sup>111</sup>In-labeled peptides was observed when combined either serum or urine at 4 °C and analyzed at 0 time.

**Biodistribution of <sup>111</sup>In-Labeled DTPA-NT Peptide Analogue (17) in Mice.** All animal studies were conducted in compliance with Mallinckrodt Medical Inc. Animal Welfare Committees' requirements for the care and use of laboratory animals in research. Established human adenocarcinoma cells (HT29, 1 × 10<sup>6</sup> cells) expressing the NT receptor were injected subcutaneously in the rear bilateral flanks of male SCID mice. The tumors grew to about 0.3 g at 14 days post implant. The tumor-bearing mice were anesthetized with Metofane gas and injected with 20 μL (10 μCi) of [<sup>111</sup>In]-DTPA-NT peptide analogue **17** (specific activity 1400 Ci/mmol) via the jugular vein. Animals (*n* = 3) were sacrificed by cervical dislocation at 1 and 4 h postinjection, and selected tissues, organs, and blood samples were collected for radioassay. Two additional animals were injected with the same amount of activity but diluted with cold NT peptide to a specific activity of 0.5 Ci/mmol. These animals were sacrificed at 2 h postinjection.

**Acknowledgment.** We thank L. Chinen for stability studies, E. G. Webb for receptor binding assays, and R. R. Wilhelm and J. Jöhler for mass spectral experiments.

## References

- (1) Friry, C.; Feliciangeli, S.; Richard, F.; Kitabgi, P.; Rovere, C. Production of recombinant large proneurotensin/neurotensin N-derived peptides and characterization of their binding and biological activity. *Biochem. Biophys. Res. Commun.* **2002**, *290*, 1161–1168.
- (2) Guha, S.; Rey, O.; Rozengurt, E. Neurotensin induces protein kinase C-dependent protein kinase D activation and DNA synthesis in human pancreatic carcinoma cell line PANC-1. *Cancer Res.* **2002**, *62*, 1632–1640.
- (3) Reubi, J. C.; Waser, B.; Schaer, J. C.; Laissue, J. A. Neurotensin receptors in human neoplasms: High incidence in Ewing's sarcomas. *Int. J. Cancer* **1999**, *82*, 213–218.
- (4) Garcia-Garayoa, E.; Blauenstein, P.; Bruehlmeier, M.; Blanc, A.; Iterbeke, K. et al. Preclinical evaluation of a new, stabilized neurotensin(8-13) pseudopeptide radiolabeled with (99m)Tc. *J. Nucl. Med.* **2002**, *43*, 374–383.
- (5) Reubi, J. C.; Waser, B.; Friess, H.; Buchler, M.; Laissue, J. Neurotensin receptors: a new marker for human ductal pancreatic adenocarcinoma. *Gut* **1998**, *42*, 546–550.
- (6) Wang, L.; Friess, H.; Zhu, Z. W.; Graber, H.; Zimmermann, A. et al. Neurotensin receptor-1 mRNA analysis in normal pancreas and pancreatic disease. *Clin. Cancer Res.* **2000**, *6*, 566–571.
- (7) Chavatte, K.; Terriere, D.; Jeannin, L.; Iterbeke, K.; Briejer, M. et al. Labeling and evaluation of new stabilised neurotensin (8-13) analogues for single photon emission tomography (SPET). *J. Label. Compd. Radiopharm.* **1999**, *42*, 423–435.
- (8) Bergmann, R.; Scheunemann, M.; Heichert, C.; Mading, P.; Wittrisch, H. et al. Biodistribution and catabolism of F-18-labeled neurotensin(8-13) analogues. *Nucl. Med. Biol.* **2002**, *29*, 61–72.
- (9) Garcia-Garayoa, E.; Allemann-Tannahill, L.; Blauenstein, P.; Willmann, M.; Carrel-Remy, N. et al. In vitro and in vivo evaluation of new radiolabeled neurotensin(8-13) analogues with high affinity for NT1 receptors. *Nucl. Med. Biol.* **2001**, *28*, 75–84.
- (10) Hong, F.; Zaidi, J.; Cusack, B.; Richelson, E. Synthesis and biological studies of novel neurotensin(8-13) mimetics. *Bioorg. Med. Chem.* **2002**, *10*, 3849–3858.
- (11) Leyton, J.; Garcia-Marin, L.; Jensen, R. T.; Moody, T. W. Neurotensin causes tyrosine phosphorylation of focal adhesion kinase in lung cancer cells. *Eur. J. Pharmacol.* **2002**, *442*, 179–186.
- (12) Lundquist, J. T. t.; Dix, T. A. Preparation and receptor binding affinities of cyclic C-terminal neurotensin (8-13) and (9-13) analogues. *Bioorg. Med. Chem. Lett.* **1999**, *9*, 2579–2582.
- (13) Lugin, D.; Vecchini, F.; Doulet, S.; Rodriguez, M.; Martinez, J. et al. Reduced peptide bond pseudopeptide analogues of neurotensin: binding and biological activities, and in vitro metabolic stability. *Eur. J. Pharmacol.* **1991**, *191*–198.
- (14) Gonzalez-Muniz, R.; Garcia-Lopez, M. T.; Gomez-Monterrey, I.; Herranz, R.; Jimeno, M. L., et al. Ketomethylene and (Cyanomethylene)amino Pseudopeptide Analogues of the C-Terminal Hexapeptide of Neurotensin. *J. Med. Chem.* **1995**, *1015*–1021.
- (15) Lundquist, J. T. t.; Bullesbach, E. E.; Golden, P. L.; Dix, T. A. Topography of the neurotensin (NT)(8-9) binding site of human NT receptor-1 probed with NT(8-13) analogues. *J. Pept. Res.* **2002**, *59*, 55–61.
- (16) Boeijen, A.; van Ameijde, J.; Liskamp, R. M. Solid-phase synthesis of oligoureic peptidomimetics employing the Fmoc protection strategy. *J. Org. Chem.* **2001**, *66*, 8454–8462.
- (17) Lundquist, J. T. t.; Dix, T. A. Synthesis and human neurotensin receptor binding activities of neurotensin(8-13) analogues containing position 8 alpha-azido-N-alkylated derivatives of ornithine, lysine, and homolysine. *J. Med. Chem.* **1999**, *42*, 4914–4918.
- (18) Kozikowski, A. P.; Dodd, D. S.; Zaidi, J.; Pang, Y.-P.; Cusack, B. et al. Synthesis of partial nonpeptidic peptide mimetics as potential neurotensin agonists and antagonists. *J. Chem. Soc., Perkin Trans. 1* **1995**, 1615–1621.
- (19) Atherton, E.; Sheppard, R. C. *Solid-phase peptide synthesis: a practical approach*; Oxford University Press: Oxford, England, 1989.
- (20) Achilefu, S.; Jimenez, H. N.; Dorshow, R. B.; Bugaj, J. E.; Webb, E. G., et al. Synthesis, in vitro receptor binding, and in vivo evaluation of fluorescein and carbocyanine peptide-based optical contrast agents. *J. Med. Chem.* **2002**, *45*, 2003–2015.
- (21) Achilefu, S.; Wilhelm, R. R.; Jimenez, H. N.; Schmidt, M. A.; Srinivasan, A. A new method for the synthesis of tri-tert-butyl diethylenetriaminepentaacetic acid and its derivatives. *J. Org. Chem.* **2000**, *65*, 1562–1565.
- (22) Gaudriault, G.; Zsurger, N.; Vincent, J. P. Compared binding properties of 125I-labeled analogues of neurotensin and neurotensin N in rat and mouse brain. *J. Neurochem.* **1994**, *361*–368.



- (23) Labbe-Jullie, C.; Blanot, D.; Morgat, J. L.; Kitabgi, P.; Checler, F. et al. Radiolabeled neurotensin analogues. II. Tritium labeled neurotensin prepared from synthetic dehydroneurotensin. *Biochimie* **1983**, 553–562.
- (24) Bruehlmeier, M.; Garayoa, E. G.; Blanc, A.; Holzer, B.; Gergely, S. et al. Stabilization of neurotensin analogues: effect on peptide catabolism, biodistribution and tumor binding. *Nucl. Med. Biol.* **2002**, 29, 321–327.
- (25) Edwards, W. B.; Fields, C. G.; Anderson, C. J.; Pajean, T. S.; Welch, M. J. et al. Generally Applicable, Convenient Solid-Phase Synthesis and Receptor Affinities of Octreotide Analogues. *J. Med. Chem.* **1994**, 37, 3749–3757.
- (26) Raynor, K.; Reisine, T. Analogues of Somatostatin Selectively Label Distinct Subtypes of Somatostatin Receptors in Rat-Brain. *J. Pharmacol. Exp. Ther.* **1989**, 251, 510–517.

JM030081K